# Mott insulators: A large class of materials for Leaky Integrate and Fire (LIF) artificial neuron

Coline Adda, Benoit Corraze, Pablo Stoliar, Pascale Diener, Julien Tranchant, Agathe Filatre-Furcate, Marc Fourmigué, Dominique Lorcy, Marie-Paule Besland, Etienne Janod, and Laurent Cario

Citation: Journal of Applied Physics **124**, 152124 (2018); doi: 10.1063/1.5042756
View online: https://doi.org/10.1063/1.5042756
View Table of Contents: http://aip.scitation.org/toc/jap/124/15
Published by the American Institute of Physics

JOURNAL OF APPLIED PHYSICS **124**, 152124 (2018)

# Mott insulators: A large class of materials for Leaky Integrate and Fire (LIF) artificial neuron

Coline Adda,[1,2] Benoit Corraze,[1] Pablo Stoliar,[2] Pascale Diener,[1] Julien Tranchant,[1] Agathe Filatre-Furcate,[3] Marc Fourmigué,[3] Dominique Lorcy,[3] Marie-Paule Besland,[1] Etienne Janod,[1] and Laurent Cario[1,a)]

[1]*Institut des Matériaux Jean Rouxel (IMN), Université de Nantes, CNRS, 2 rue de la Houssinière, BP 32229, 44322 Nantes Cedex 3, France*

[2]*CIC nanoGUNE, Tolosa Hiribidea 76, 20018 Donostia-San Sebastian, Spain*

[3]*Univ Rennes, CNRS, ISCR (Institut des Sciences Chimiques de Rennes)-UMR 6226, 35 042 Rennes, France*

(Received 4 June 2018; accepted 18 August 2018; published online 8 October 2018)

A major challenge in the field of neurocomputing is to mimic the brain's behavior by implementing artificial synapses and neurons directly in hardware. Toward that purpose, many researchers are exploring the potential of new materials and new physical phenomena. Recently, a new concept of the Leaky Integrate and Fire (LIF) artificial neuron was proposed based on the electric Mott transition in the inorganic Mott insulator $GaTa_4Se_8$. In this work, we report on the LIF behavior in simple two-terminal devices in three chemically very different compounds, the oxide $(V_{0.89}Cr_{0.11})_2O_3$, the sulfide $GaMo_4S_8$, and the molecular system [Au(iPr-thiazdt)$_2$] ($C_{12}H_{14}AuN_2S_8$), but sharing a common feature, their Mott insulator ground state. In all these devices, the application of an electric field induces a volatile resistive switching and a remarkable LIF behavior under a train of pulses. It suggests that the Mott LIF neuron is a general concept that can be extended to the large class of Mott insulators. *Published by AIP Publishing.* https://doi.org/10.1063/1.5042756

## I. INTRODUCTION

Since the early 2000s, artificial intelligence has grown tremendously due to the development of artificial neural networks (ANNs) that allow one to mimic the brain's behavior and to solve some problems such as data mining or pattern recognition.[1] These neural networks are mostly implemented in software on computers using the von Neumann architecture.[2] As a consequence, they suffer from the main drawback of this architecture, i.e., the energy consumption. A much more energy-efficient solution consists in implementing the neural network directly in hardware,[3–6] using both artificial neurons and synapses. Since 2015, some big industries like IBM or Intel developed artificial neural network directly in hardware using the CMOS technology with a huge number of transistors to produce neurons and synapses. For instance, IBM TrueNorth[3] uses $5.4 \times 10^9$ transistors to mimic $1 \times 10^6$ neurons and $256 \times 10^6$ synapses. To reduce the circuit complexity, a big step forward would be to fabricate simple devices made of two elementary blocks: single component neurons and synapses. In the last decade and following the discovery of "memristors,"[7–9] many efforts have been devoted to the search of a single component artificial synapse.[10] In comparison, the research for single component artificial neurons was struggling to start. This is likely due to the complex behavior of neuron that cannot be easily mimicked using physical properties of existing materials used in microelectronics. For this reason, new classes of materials (namely, spintronic materials, memristors, and Mott insulators) have begun to be investigated by virtue of their nonlinear electrical behavior capable of reproducing the neuron's functionalities.[11,12] The first progress was achieved with the "neuristor" implementing the Hodgkin–Huxley model of artificial neuron[13] and exploiting the nonlinear behavior of $NbO_2$ memristors associated with a thermally driven transition.[14] Although the neuristor represented a real simplification of the artificial neuron architecture, it is still composed of several resistances, $NbO_2$ memristors, and capacitors. A further simplification was recently achieved exploiting the nonlinear behavior of oxide memristors (also called threshold switching).[15,16] Alternatively, magnetic tunnel junctions were also proposed to build up single component artificial neurons. These spintronic devices exhibit indeed a nonlinear electrical behavior leading to oscillatory regimes that were used to implement an artificial neuron.[17] Finally, it was suggested that a two-terminal device made of the Mott insulator $GaTa_4Se_8$ could implement the Leaky Integrate and Fire (LIF) model of artificial neuron[18] thanks to its nonlinear behavior. Under electric field, $GaTa_4Se_8$ exhibits indeed a collapse of the Mott insulating state at the local scale leading to a resistive switching and a remarkable LIF behavior. This phenomenon called electric Mott transition was universally observed in Mott insulators[19] which gives hope that the LIF behavior could also be a general feature of these compounds. This would expand materials available for the realization of artificial LIF Neuron to the large class of Mott insulators. Here, we show that the LIF behavior can be indeed observed in oxide $(V_{1-x}Cr_x)_2O_3$ and sulfide $GaMo_4S_8$ inorganic Mott insulators, as well as in the molecular [Au(R-thiazdt)$_2$] (R = iPr) gold dithiolene complex. This work is therefore a proof of principle that all Mott insulators can be considered as a LIF single component artificial neuron.

a)E-mail: laurent.cario@cnrs-imn.fr

## II. METHODS

$(V_{0.89}Cr_{0.11})_2O_3$ crystals were prepared by mixing $V_2O_5$ (Aldrich, >99.6%) and $Cr_2O_3$ (Prolabo, 99.9%) powders. $V_2O_5$ powder was mixed with $Cr_2O_3$ in the 0.85: 0.15M ratio after a first drying at 400 °C. The mixture was then baked in an oven at 900 °C for 10 h under a 95% Ar–5% $H_2$ gas flow. Half a gram of obtained $(V_{0.85}Cr_{0.15})_2O_3$ powder was then introduced in a silica tube, with 40 mg of sulfur as a vapor phase transport agent. The tube was vacuum sealed, heated up to 1050 °C in a temperature gradient (≈10 °C/cm) furnace, and then cooled down at −2 °C/h to 900 °C, before a faster cooling (−300 °C/h) to room temperature.

$GaMo_4S_8$ crystals were prepared[20] using a mixture of molybdenum (Mo), molybdenum sulfide ($MoS_2$), and gallium sulfide ($Ga_2S_3$). The initial stoichiometry $Ga_{20}Mo_{35}S_{45}$ (corresponding to $Ga_{3,33}Mo_4S_{5,14}$), different from the targeted composition, was optimized to obtain large single crystals (between 150 $\mu$m and 1 mm) of $GaMo_4S_8$. The mixture was then pressed into a pellet, loaded in an alumina crucible, and introduced in a molybdenum crucible which was sealed in an electric arc furnace under partial pressure of argon. The molybdenum crucible was then heated up quickly at 900 °C $h^{-1}$ to 1600 °C, held at this temperature during 5 min, cooled down slowly, first to 1480 °C at 60 °C $h^{-1}$, then to 1000 °C at 100 °C $h^{-1}$, and finally to room temperature at 30 °C $h^{-1}$. Large octahedral $GaMo_4S_8$ crystals (typical size >500 $\mu$m) were isolated from their gangue by dissolution of GaS and $GaMo_3$ in aqua media.

The neutral radical gold dithiolene complex [Au(iPr-thiazdt)2] belongs to a broad family of radical gold dithiolene complexes showing a Mott insulator behavior.[21–24] This compound was obtained as single crystals upon electrocrystallization in $CH_3CN$ of its monoanionic precursor, $[Au(iPr\text{-}thiazdt)2]^-$ as $Ph_4P^+$ salt in the presence of an excess of $nBu_4NPF_6$ upon application of a constant current of 0.4 $\mu$A for 10 days [20]. For this study, all single crystals were selected from the same batch.

For electrical characterization, Mott insulator crystals have been contacted with 17 $\mu$m gold wires using a carbon paste (Electrodag PR-406) and then annealed in vacuum at 150 °C for 20 min to achieve a low contact resistance. The low-bias resistance was measured using a high-impedance Keithley 236 source-measure unit. Mott insulators crystals were connected in series with a load resistance $R_{load}$ playing the role of current limiter and ranging in the 5%-10% of the sample resistance. All voltage pulses were applied using an Agilent 81150A pulse function generator.

## III. ELECTRIC MOTT TRANSITION AND LIF BEHAVIOR

During the last few years, numerous experiments have demonstrated that a Mott insulator subjected to an electric field exceeding a threshold value undergoes an insulator to metal transition at the local scale. This phenomenon called electric Mott transition is a universal property of Mott insulators.[19,25–29]

Figure 1 schematized the electric Mott transition and concomitant resistive switching during an electric pulse. Above a threshold electric field, free carriers are accelerated within the Mott insulators, which enhances the electronic temperature and promote the massive creation of new carriers.[30] This phenomenon leads to an electronic avalanche breakdown which induces the formation of a metallic filamentary path within the material after a time delay ($t_{delay}$) which varies as the inverse of the applied voltage [Figs. 1(a) and 1(b)]. The resistive switching occurs when the filamentary path bridges the opposite electrodes [Figs. 1(c)–1(f)]. Once this filamentary path is created, two situations may be encountered after the end of the voltage pulse as depicted in Figs. 1(g) and 1(h). The filamentary path can either fully or only partially dissolve. In the last situation, the resistance does not relax back to its initial value, if the remaining filamentary path percolates between electrodes. This type of resistive switching is called non-volatile and is usually obtained when the applied voltage is large compared to the threshold voltage. Conversely, when the filament self dissolves, the resistance relaxes back to its initial value, and for this reason, this type of resistive switching is called volatile. This volatile resistive switching is usually observed for voltages slightly higher than the threshold field. Recently, it was proposed that the stability of the filamentary path could be related to elastic constraints and that below a critical size the filamentary path could not be stable by itself and would completely dissolve, whereas larger filaments would be metastable.[31]

To capture the main features of the Electric Mott Transition, a phenomenological model was developed. The method and main results of this work were published elsewhere.[18] Under electric field, some hot carriers are produced that break locally the Mott insulating state and generate a correlated metal (CM) phase. To account for the competition between the two phases under electric field, a two-minima energy landscape, where the Mott insulator (MI) state is at the lowest energy and the correlated metal (CM) state at higher energy [see Figs. 2(a) and 2(b)], was considered and implemented in a resistor network [see Fig. 2(c)]. At equilibrium, the system is in the MI state, the CM state being a metastable state at energy $E_M$ above that of the MI state. Due to the energy barrier $E_B$ between the two states, the probability for the system to jump into the CM state, noted $P_{MI\rightarrow CM}$ in Eq. (1), is close to zero without electric field. However, the application of an electric field will destabilize the MI state increasing its energy level by (qΔV) [(see Fig. 2(a)], and thus, the probability for the system to jump into the CM state will increase. The probability to come back into the MI state, noted $P_{CM\rightarrow MI}$ in Eq. (2), is just thermally activated, the system relaxing from the metastable state [see Fig. 2(b)].

$$P_{MI\rightarrow CM} = c * \exp\left(-\frac{E_B - q|\Delta V|}{k_B T}\right), \quad (1)$$

$$P_{CM\rightarrow MI} = c * \exp\left(-\frac{E_B - E_M}{k_B T}\right), \quad (2)$$

where $c$ is a constant, $E_B$ is the energy barrier, $q$ is the charge, $T$ is the temperature, and $\Delta V$ is the local voltage drop for the system.

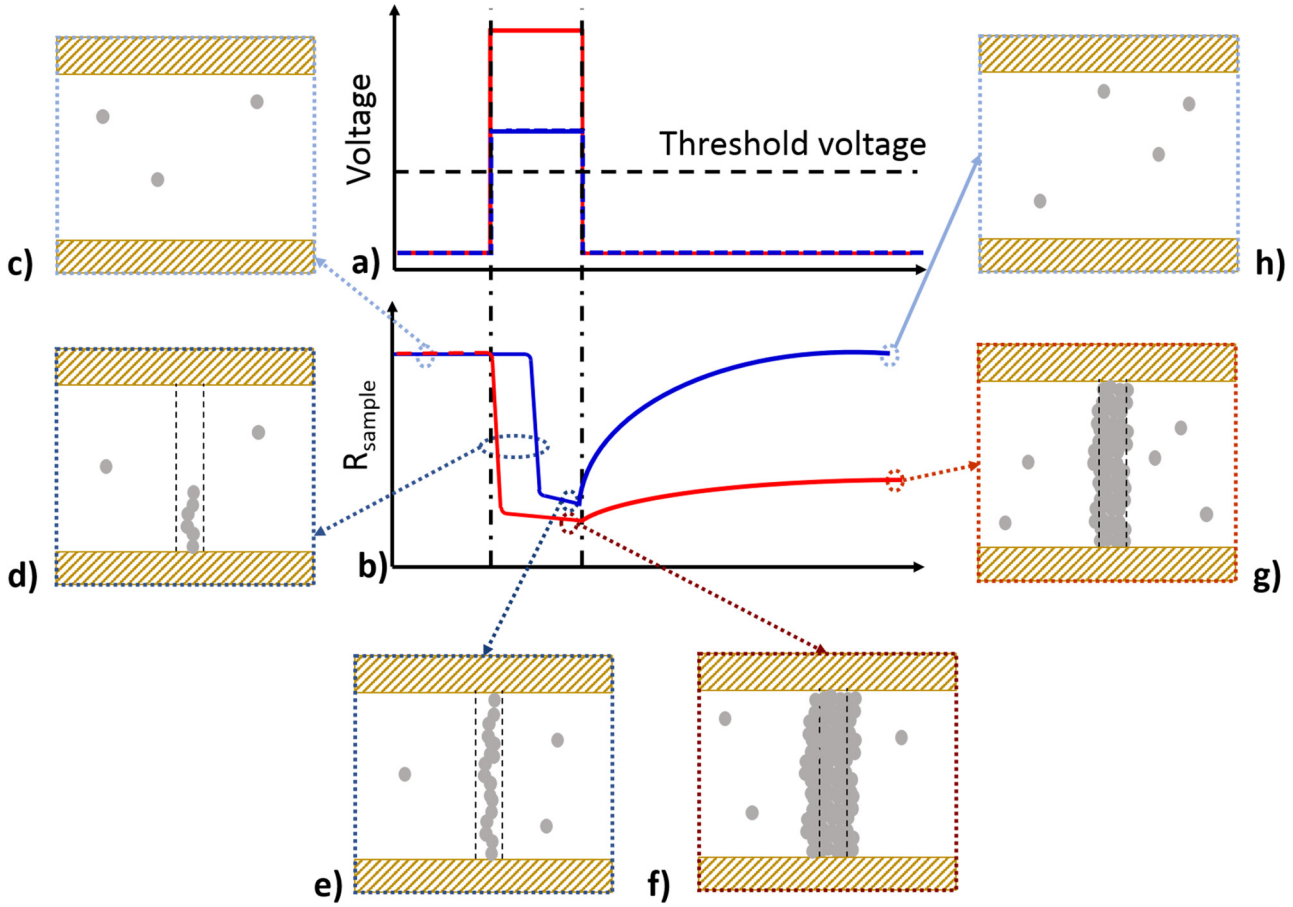


FIG. 1. Schematic representation of the electric Mott transition. (a) Voltage pulse applied on the Mott insulator. The blue and red pulse correspond to different voltages above the threshold voltage. (b) Variation of the sample resistance before, during, and after the voltage pulses. Before the voltage pulse, the sample resistance is in the high resistive state. During the voltage pulse, resistive switching to low resistive states is observed after a delay time which decrease with increasing voltage. After the pulse, the sample resistance either returns to its initial value, (blue curve) meaning that the resistive switching is volatile, or the sample resistance remains in the low resistance state, leading hence to a non-volatile resistive switching. [(c)–(h)] Snapshots correspond to the time evolution of the formation of the metallic filamentary path within the sample associated with the resistive switching. The brown hatched rectangles represent the electrodes.

According to the model, the fraction $n_{CM}$ of metallic sites within the resistor network under series of pulses evolves according to Eq. (3).

$$\frac{\partial}{\partial t} n_{CM} = -n_{CM} P_{CM \to MI} + p(t) N^{-1} \sum_{MI\ cells} P_{MI \to CM}. \qquad (3)$$

The first term in Eq. (3) describes the relaxation of CM cells back to the MI cells (leaky term), and the second term accounts for the switching of MI cells to the CM state (integration term); $p(t) = 1$ during the voltage pulses and $p(t) = 0$ otherwise ensures that the creation of metallic sites occurs only during the voltage pulse. During the pulse, the model predicts that sparsely isolated metallic cells form first, and that the fraction $n_{CM}$ increases linearly with time. For moderate applied electric fields, the fraction $n_{CM}$ eventually saturates at a very diluted value ($n_{CM} \ll 0.01$), leading to a negligible reduction of the sample resistance. An important outcome of this model is the prediction of a threshold fraction $n_{CM}$*, reached above a threshold electric field $E_{th}$. For fields exceeding $E_{th}$, the temporal evolution of the metallic fraction $n_{CM}$ becomes non-linear, and a steep increase of $n_{CM}$ is observed after a time delay $t_{delay}$, associated with the creation of a metallic filamentary path bridging the electrodes.[18] This phenomenon is associated with a sudden drop of the electrical resistance.

Interestingly, this model can easily describe the response of the system to the application of a train of short pulses. Figure 2(d) sketches the main results of such a modelling for pulse duration shorter than $t_{delay}$, which finally lead also to a resistive switching. The fraction of metallic sites increases during each pulses, but relax between them. For inter-pulse duration shorter than this relaxation process, the fraction of metallic sites steadily increases from pulse to pulse. When the fraction of metallic sites $n_{CM}$ reaches the threshold value $n_{CM}$*, the percolating filament is created between the electrodes, provoking a burst of current into the circuit called firing.[3] Mott insulator may therefore be viewed as leaky integrators of metallic sites. This modelling work points therefore to a remarkable feature of Mott insulators: they implement the three functionalities of Leaky Integrate and Fire under electric field.

## IV. LEAKY INTEGRATE AND FIRE ARTIFICIAL NEURONS REALIZED UNIVERSALLY WITH MOTT INSULATORS

Neurons in the mammal brain fulfill three main functions called Leaky Integrate and Fire. The neurons receive electric

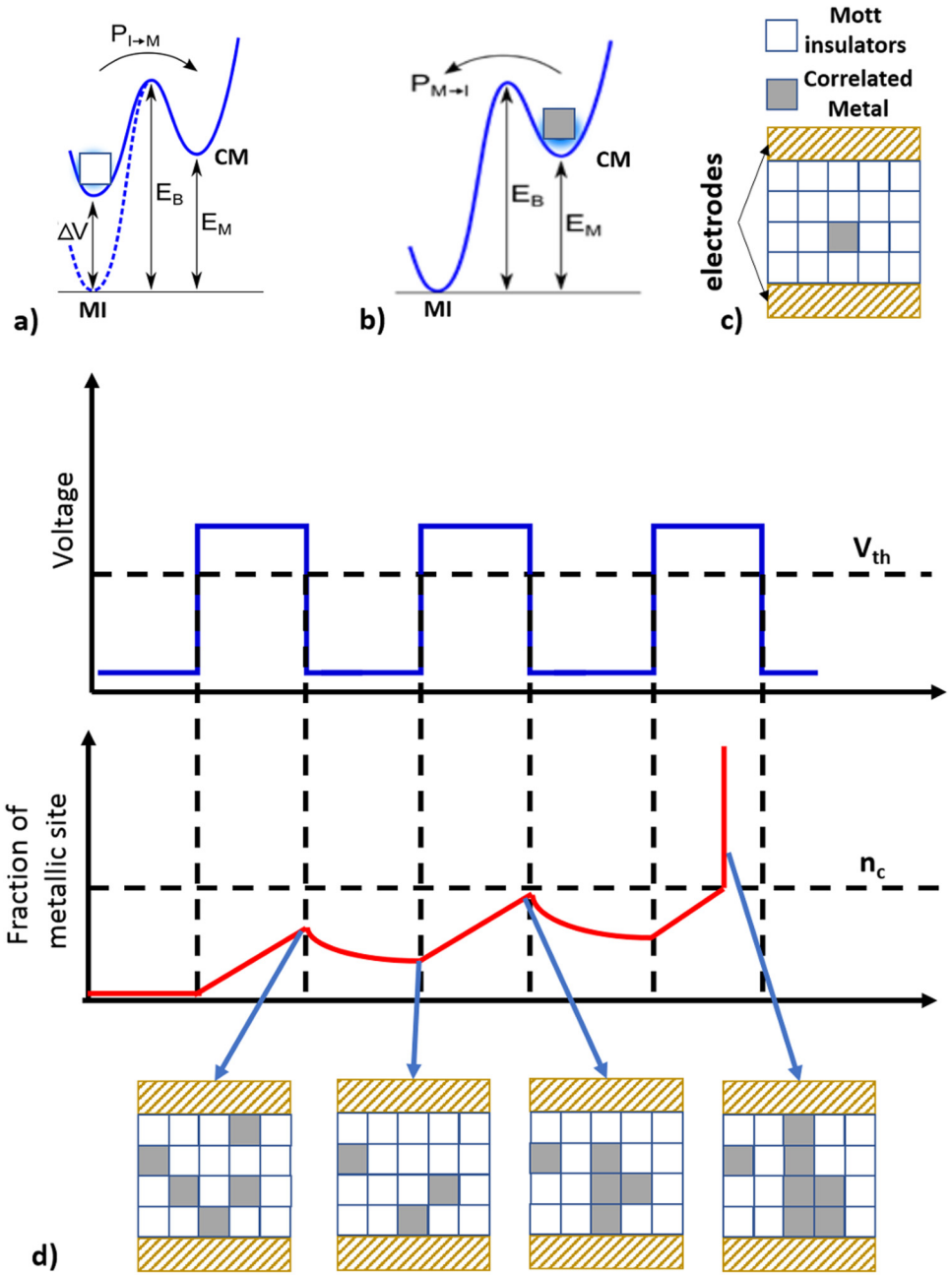


FIG. 2. Schematic of the Leaky Integrate and Fire. [(a), (b)] Energy diagram of Mott insulator and correlated metal states. (a) The probability to induce the Mott insulator-metal transition is driven by an external electric field. (b) The probability for the transited site to relax is thermally activated. (c) Resistor network represents Mott insulators. Each cell models a little fraction of Mott insulator. The two brown hatched rectangle represents electrodes. (d) Simulated evolution of fraction of metallic sites in the resistor network. During the voltage pulses, the fraction of metallic sites increases in the resistor network. Between two voltage pulses, some transited sites collapse. During the fourth pulse, the critical fraction of the metallic site is reached, above which a metallic filamentary path bridging the electrodes is created, inducing the resistive transition.

pulses coming from other neurons, which contribute to enhance their membrane potential (integrate function). The membrane potential relaxes between incoming pulses, a feature called "Leaky." Above a threshold value of the membrane, the neuron emits an action potential toward other neurons, an event called "Fire." Lapicque already realized in 1907 that the neuron behaves like a parallel RC circuit before the Fire event. His model, called Leaky Integrate and Fire (LIF), states that incoming spikes will charge the capacitor with electrical charges, which will then "leak" through the resistor in parallel.[32,33] When the membrane potential reaches a given threshold, the neuron fires an output electric spike. Interestingly, artificial neural networks (ANNs) using discrete spikes to compute and transmit information (Spiking Neural Networks) are technologically appealing thanks to their high energy efficiency; the building block of such ANNs is usually a Leaky Integrate and Fire neuron.[34]

Comparing the behavior of the Neuron and of the Mott insulator under electric field suggests a straightforward analogy. In a Mott insulator, the accumulation of correlated metal sites might play a similar role as the accumulation of charges in the cellular membrane of the neuron. The Electric Mott transition is therefore of great interest in the context of neurocomputing as it opens a unique opportunity to implement the Leaky Integrate and Fire (LIF) functionalities and build up a LIF artificial neuron.

So far, the LIF behavior was demonstrated on crystals of $GaTa_4Se_8$ Mott insulator.[18] In order to check the generality of this behavior, we have looked for LIF behavior in other Mott insulators. For this demonstration, we have chosen three different compounds among oxide, sulfide, and molecular Mott insulators, namely $(V_{0.89}Cr_{0.11})_2O_3$, $GaMo_4S_8$, and [Au(iPr-thiazdt)$_2$] whose structures are represented in Figs. 3(a), 3(e), and 3(i), respectively. Crystals of these

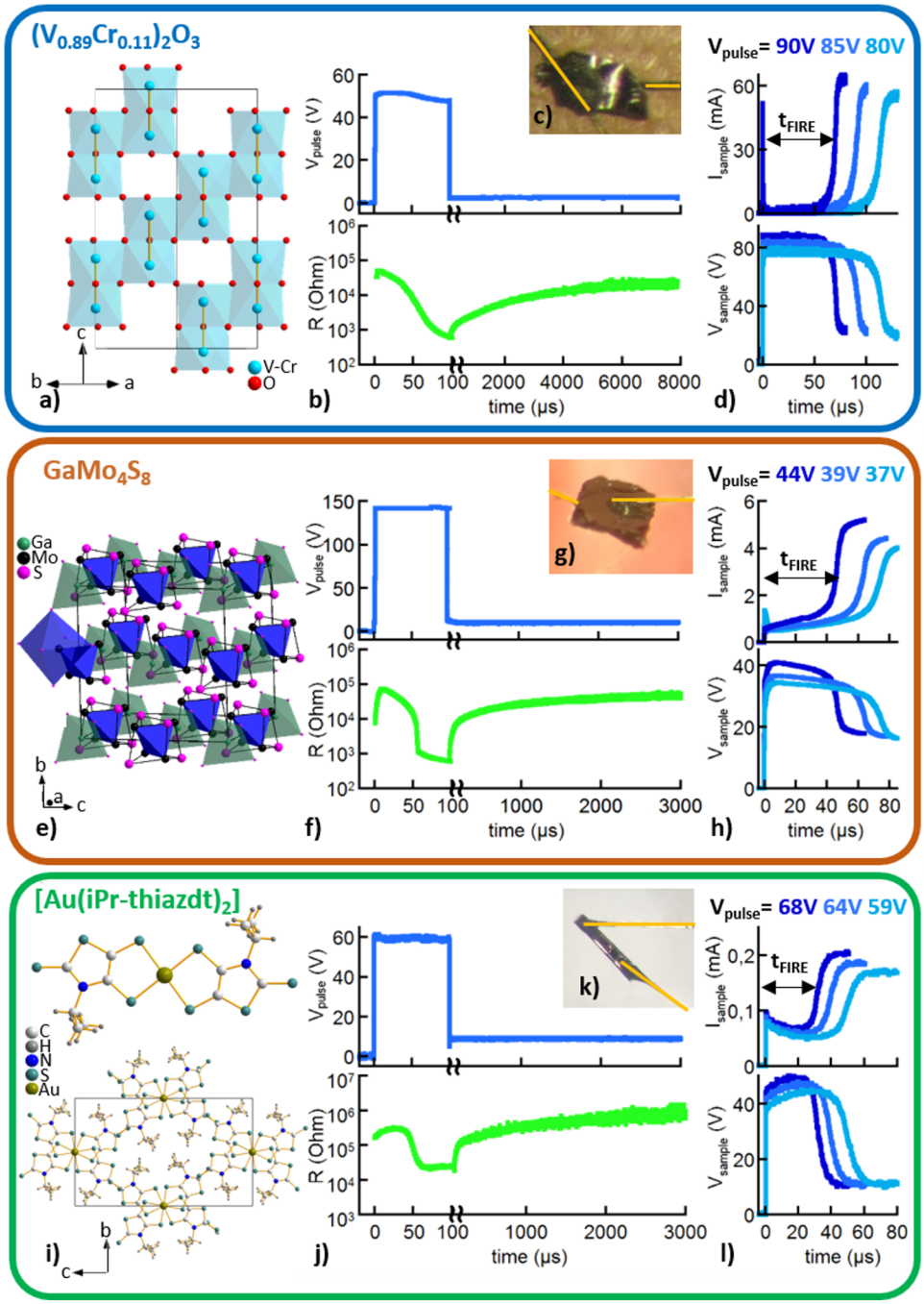


FIG. 3. Presentation of the crystallographic structure, behavior under electric pulse, and picture of single crystals used in this work of [(a)–(d)] inorganic $(V_{0.89}Cr_{0.11})_2O_3$ Mott insulator (blue frame), [(e)–(h)] inorganic $GaMo_4S_8$ Mott insulator (orange frame), [(i)–(l)] organic [Au(iPr-thiazdt)$_2$] ($C_{12}H_{14}AuN_2S_8$) Mott insulator (green frame). [(a), (e), (i)] Crystallographic structures. [(b), (f), (j)] A resistive switching occurs under an electric pulse of 100 $\mu$s. The resistance switches from a high resistive state to a low resistive state after a delay of roughly 50 $\mu$s. After the pulse, an applied low bias voltage allows one to measure the relaxation of the resistance up to its initial value. [(c), (g), (k)] Picture of $(V_{0.89}Cr_{0.11})_2O_3$ crystal slice, $GaMo_4S_8$ crystal slice, and [Au(iPr-thiazdt)$_2$] crystal. Voltage is applied through gold wire (highlight with yellow line is the pictures) pasted on the crystals. [(d), (h), (l)] Time dependence of the voltage across the different crystals for several voltages applied to the circuit. Above a threshold voltage of ≈19 V at 164 K (equivalent to 6 kV/cm) for $(V_{0.89}Cr_{0.11})_2O_3$, a threshold voltage of ≈16 V at 74 K (equivalent to 3.5 kV/cm) for $GaMo_4S_8$, and a threshold voltage of ≈13 V at 64 K (equivalent to 3 kV/cm) for [Au(iPr-thiazdt)$_2$], a resistive switching occurs after a delay time which decreases when the sample voltage (applied electric pulse) increases.

compounds were synthesized as described in the method part and then contacted with two electrodes as shown in Figs. 3(c), 3(g), and 3(k). Volatile resistive switching was observed under electric pulses for all these devices, that is, for $(V_{0.89}Cr_{0.11})_2O_3$ at 164 K [Figs. 3(b) and 3(d)], for $GaMo_4S_8$ at 74 K [Figs. 3(f) and 3(h)], and for [Au(iPr-thiazdt)$_2$] at 60 K [Figs. 3(j) and 3(l)]. As shown in these figures, each voltage pulse which exceeds the threshold value (of the order of a few kV/cm) induces a volatile resistive switching and a burst of current into the circuit, i.e., a firing event. All these switchings are volatile, and an exponential-like relaxation is observed for all compounds after the electric pulse as revealed by Figs. 3(b), 3(f), and 3(j). Moreover, the delay time $t_{FIRE}$ decreases upon increasing applied voltage as confirmed by Figs. 3(d), 3(h), and 3(l).

These resistive switching and relaxation observed using single pulses give a clear demonstration of the Electric Mott Transition in $(V_{0.89}Cr_{0.11})_2O_3$, $GaMo_4S_8$, and [Au(iPr-thiazdt)$_2$] and strongly suggest that a LIF behavior may be also achieved in these compounds. To confirm this assertion, Fig. 4 shows the behavior of $(V_{0.89}Cr_{0.11})_2O_3$, $GaMo_4S_8$, and [Au(iPr-thiazdt)$_2$] under train of short pulses. When the $(V_{0.89}Cr_{0.11})_2O_3$ crystal slice [blue frame in Fig. 4(a)] receives a series of pulse of a duration $t_{ON} = 40\,\mu$s separated by a time interval of $t_{OFF} = 30\,\mu$s, it undergoes a volatile resistive switching during the second pulse ($N_{FIRE} = 2$) after a cumulated time under a voltage of roughly ≈60 $\mu$s. If $t_{ON}$ is now decreased from 40 to 30 $\mu$s letting less time during each pulse for accumulation of metallic sites, the number of pulses required to observe the Fire $N_{FIRE}$ increases

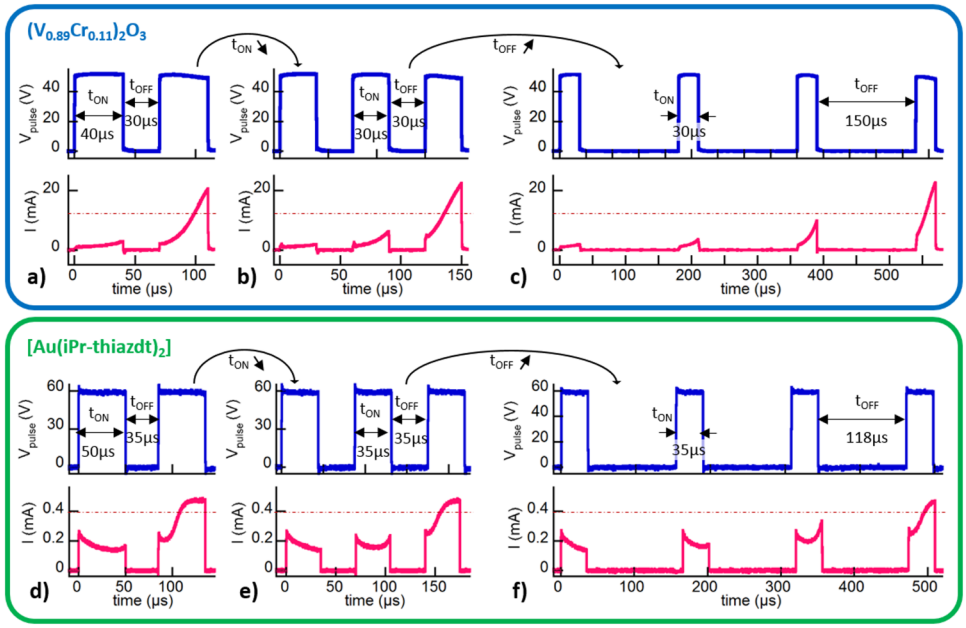


FIG. 4. Train of pulses of various $t_{ON}$ and $t_{OFF}$ applied on $(V_{0.89}Cr_{0.11})_2O_3$ 164 K (blue frame) and [Au(iPr-thiazdt)$_2$] at 60 K (green frame) Mott insulators. On $(V_{0.89}Cr_{0.11})_2O_3$, (a) using $t_{ON} = 40\,\mu s$ and $t_{OFF} = 30\,\mu s$ leads to $N_{FIRE} = 2$. (b) Decreasing $t_{ON}$ to $30\,\mu s$ leads to increase $N_{FIRE}$ to 3. (c) Increasing $t_{OFF}$ to $150\,\mu s$ leads to increase $N_{FIRE}$ to 4. On [Au(iPr-thiazdt)$_2$], (d) using $t_{ON} = 50\,\mu s$ and $t_{OFF} = 35\,\mu s$ leads to $N_{FIRE} = 2$. (e) Decreasing $t_{ON}$ to $35\,\mu s$ leads to increase $N_{FIRE}$ to 3. (f) Increasing $t_{OFF}$ to $118\,\mu s$ leads to increase $N_{FIRE}$ to 4. These experiments demonstrate that the Leaky Integrate and Fire behavior can be found universally in Mott insulators whether they are organic or inorganic. Furthermore, $N_{FIRE}$, thus the Leaky Integrate and Fire behavior, can be controlled by the applied train of pulses.

from 2 to 3 and the cumulated time under voltage increases to $\approx 75\,\mu s$ [see Fig. 4(b)]. This experiment clearly demonstrates a cumulative effect (Integrate functionality) which is not perfect (Leaky functionality). The Leaky feature is further confirmed by increasing the time interval between two pulses from $t_{OFF} = 30\,\mu s$ to $t_{OFF} = 150\,\mu s$, thus giving more time for the relaxation of metallic sites. In this case, $N_{FIRE}$ increases from 3 to 4, after a cumulated time close to $100\,\mu s$ [see Fig. 4(c)].

Similar conclusions may be drawn in the case of the [Au(iPr-thiazdt)$_2$]. Figure 4(d) displays the behavior of this compound under pulse trains. For a series of pulses of a duration $t_{ON} = 50\,\mu s$ separated by a time interval $t_{OFF} = 35\,\mu s$, a resistive switching occurs during the second pulse, i.e., after a cumulated time under voltage of $\approx 65\,\mu s$. When decreasing $t_{ON}$ from 50 to $35\,\mu s$, an increase of $N_{FIRE}$ to 3 is observed; the firing event occurs after a cumulated time close to $80\,\mu s$ [Fig. 4(e)] which is larger than under the previous conditions and demonstrates an imperfect accumulation. The Leaky effect is confirmed by increasing the time interval between two pulses from $t_{OFF} = 35\,\mu s$ to $t_{OFF} = 118\,\mu s$ [see Fig. 4(f)]. In this case, the number of pulses required to reach the firing event increases from 3 to 4.

These experiments on $(V_{0.89}Cr_{0.11})_2O_3$ and [Au(iPr-thiazdt)$_2$] confirm the LIF behavior of both compounds and highlight that a full control of the LIF behavior may be achieved by tuning the pulse train parameters. It may be understood on the basis of Eq. (2) of our model as the number of pulses required to reach the firing event $N_{FIRE}$ depends on the production and destruction rates of metallic sites. For this reason, $N_{FIRE}$ depends directly on the parameters $t_{ON}$ and $t_{OFF}$ of the pulse train as they change the balance between the production and destruction of metallic sites. So far, all experiments were performed with a voltage set to 0 during $t_{OFF}$, meaning that the production rate is null during that time. However, as of today, we do not know how far the applications of the Mott LIF neuron in artificial neural networks can go. Depending on these potential applications, several control parameters could be privileged. It is therefore important to prospect on different ways to control the Leaky Integrate and Fire Mott neuron. An alternative way to tune

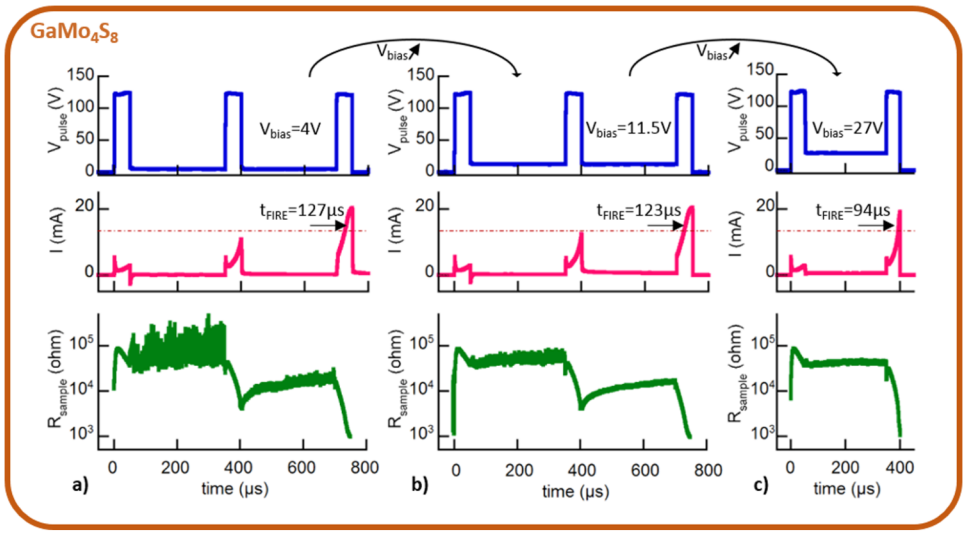


FIG. 5. Train of pulses with $t_{ON} = 50\,s$ and $t_{OFF} = 300\,\mu s$ and various bias voltage between pulses applied on $GaMo_4S_8$. (a) Using $V_{bias} = 4\,V$ leads to $N_{FIRE} = 3$. Between pulses, the resistance relaxes until the next pulse. (b) Increasing $V_{bias}$ to 11.5 V leads to a decrease of $t_{FIRE}$ of $4\,\mu s$ during the same $N_{FIRE}$ (= 3) and a decrease of the relaxation of the resistance between pulses. (c) Increasing $V_{bias}$ to 27 V leads to the decrease of $N_{FIRE}$ to 2. The relaxation of the resistance is almost zero between two pulses.

the ratio between the production and destruction rate of metallic sites could be therefore to use a voltage bias during $t_{OFF}$ allowing therefore for a small production rate during that time. To test this hypothesis, experiments with a bias voltage applied during $t_{OFF}$ were carried out on a $GaMo_4S_8$ crystal slice and are displayed in Fig. 5. In all these experiments, the $GaMo_4S_8$ crystal slice receives a series of pulse of 120 V, with a duration $t_{ON} = 50\,\mu s$ separated by a time interval of $t_{OFF} = 300\,\mu s$. During the inter-pulse time $t_{OFF}$, a bias voltage $V_{bias}$ is applied with different values below or above the threshold voltage $V_{th} \approx 17$ V observed for the device. In Fig. 5(a), a low $V_{bias}$ of 4 V is applied during the inter-pulse time $t_{OFF}$. In these conditions, the resistive switching occurs during the third pulse. Increasing $V_{bias}$ to 11.5 V does not change $N_{FIRE}$ [see Fig. 5(b)], but the time required under voltage to reach the firing event is reduced by about 4 $\mu s$. In the same time, a smaller relaxation of the resistance is observed compared to the previous case with $V_{bias} = 4$ V. Finally, increasing $V_{bias}$ to 27 V leads to a decrease of $N_{FIRE}$ to 2 [see Fig. 5(c)]. In this case, $V_{bias}$ is over the threshold voltage, and as expected, the resistance does no longer relax during $t_{OFF}$. All these observations confirm the LIF behavior in the sulfide Mott insulator $GaMo_4S_8$ and demonstrate that a full control of the LIF behavior may be achieved by tuning the pulse train parameters, namely $t_{ON}$, $t_{OFF}$, $V_{pulse}$, and $V_{bias}$.

## V. CONCLUSION

We have demonstrated that the three Mott insulators, $(V_{0.89}Cr_{0.11})_2O_3$, [Au(iPr-thiazdt)$_2$], and $GaMo_4S_8$, exhibit an electric Mott transition leading to a Leaky Integrate and Fire behavior. As a consequence, we may infer that these functionalities can be universally observed in the large class of Mott insulators, regardless of their molecular or inorganic nature. Therefore, this opens a large choice of materials for the realization of LIF artificial neurons based on the electric Mott transition. However, to be implemented into neuromorphic hardware, the materials have to be deposited in thin films. A first thin film device was realized recently.[35] On this device, the LIF behavior was observed at higher temperature thanks to the increase of sample resistance. Reducing the thin film thickness will allow one to increase further their resistance which may lead to obtaining artificial neurons operating at room temperature. Moreover, reducing inter-electrode distances should allow one to reduce the used voltages and to reduce the power consumption, as was already demonstrated for the non-volatile resistive switching.[29]

## ACKNOWLEDGMENTS

The authors thank the "Région Pays de la Loire" for funding the present work in the framework of the "Pari scientifique Neuro-Mott." P.S. acknowledges the support of the Spanish Ministry of Economy through the Ramón y Cajal (Grant No. RYC-2012-01031). This work was also supported by the ANR (France) under project GOLD-RRAM No. 12-BS07-0032. We also thank the Rennes-Nantes Materials Program supported jointly by CNRS, the Universities of Rennes and Nantes, and the Régions Bretagne and Pays de la Loire for supporting the post-doctoral fellowship of P.D.

[1]A. K. Jain, J. Mao, and K. M. Mohiuddin, Computer **29**, 31 (1996).
[2]D. Baptista, S. Abreu, F. Freitas, R. Vasconcelos, and F. Morgado-Dias, Neural Comput. Appl. **23**, 591 (2013).
[3]P. A. Merolla, J. V. Arthur, R. Alvarez-Icaza, A. S. Cassidy, J. Sawada, F. Akopyan, B. L. Jackson, N. Imam, C. Guo, Y. Nakamura, B. Brezzo, I. Vo, S. K. Esser, R. Appuswamy, B. Taba, A. Amir, M. D. Flickner, W. P. Risk, R. Manohar, and D. S. Modha, Science **345**, 668 (2014).
[4]J. J. Yang, D. B. Strukov, and D. R. Stewart, Nat. Nanotechnol. **8**, 13 (2013).
[5]G. Indiveri, B. Linares-Barranco, T. J. Hamilton, A. van Schaik, R. Etienne-Cummings, T. Delbruck, S.-C. Liu, P. Dudek, P. Häfliger, S. Renaud, J. Schemmel, G. Cauwenberghs, J. Arthur, K. Hynna, F. Folowosele, S. Saighi, T. Serrano-Gotarredona, J. Wijekoon, Y. Wang, and K. Boahen, Front. Neurosci. **5**, 73 (2011).
[6]Nature **554**, 145 (2018).
[7]L. Chua, Appl. Phys. A **102**, 765 (2011).
[8]S. H. Jo, T. Chang, I. Ebong, B. B. Bhadviya, P. Mazumder, and W. Lu, Nano Lett. **10**, 1297 (2010).
[9]D. Kuzum, S. Yu, and H.-S. Philip Wong, Nanotechnology **24**, 382001 (2013).
[10]D. B. Strukov, G. S. Snider, D. R. Stewart, and R. S. Williams, Nature **453**, 80 (2008).
[11]Y. Yang and W. Lu, Nanoscale **5**, 10076 (2013).
[12]D. S. Jeong, I. Kim, M. Ziegler, and H. Kohlstedt, RSC Adv. **3**, 3169 (2013).
[13]M. D. Pickett, G. Medeiros-Ribeiro, and R. S. Williams, Nat. Mater. **12**, 114 (2012).
[14]V. Eyert, EPL **58**, 851 (2002).
[15]A. Mehonic and A. J. Kenyon, Front. Neurosci. **10** (2016).
[16]S. Kumar, J. P. Strachan, and R. S. Williams, Nature **548**, 318 (2017).
[17]J. Torrejon, M. Riou, F. A. Araujo, S. Tsunegi, G. Khalsa, D. Querlioz, P. Bortolotti, V. Cros, K. Yakushiji, A. Fukushima, H. Kubota, S. Yuasa, M. D. Stiles, and J. Grollier, Nature **547**, 428 (2017).
[18]P. Stoliar, J. Tranchant, B. Corraze, E. Janod, M.-P. Besland, F. Tesler, M. Rozenberg, and L. Cario, Adv. Funct. Mater. **27**, 1604740 (2017).
[19]E. Janod, J. Tranchant, B. Corraze, M. Querré, P. Stoliar, M. Rozenberg, T. Cren, D. Roditchev, V. T. Phuoc, M.-P. Besland, and L. Cario, Adv. Funct. Mater. **25**, 6287 (2015).
[20]M. Querré, B. Corraze, E. Janod, M.-P. Besland, J. Tranchant, M. Potel, S. Cordier, V. Bouquet, M. Guilloux-Viry, and L. Cario, Key Eng. Mater. **617**, 135 (2014).
[21]N. Tenn, N. Bellec, O. Jeannin, L. Piekara-Sady, P. Auban-Senzier, J. Iñiguez, E. Canadell, and D. Lorcy, J. Am. Chem. Soc. **131**, 16961 (2009).
[22]G. Yzambart, N. Bellec, G. Nasser, O. Jeannin, T. Roisnel, M. Fourmigué, P. Auban-Senzier, J. Íñiguez, E. Canadell, and D. Lorcy, J. Am. Chem. Soc. **134**, 17138 (2012).
[23]B. Brière, J. Caillaux, Y. Le Gal, D. Lorcy, S. Lupi, A. Perucchi, M. Zaghrioui, J. C. Soret, R. Sopracase, and V. Ta Phuoc, Phys. Rev. B **97**, 035101 (2018).
[24]A. Filatre-Furcate, T. Roisnel, M. Fourmigué, O. Jeannin, N. Bellec, P. Auban-Senzier, and D. Lorcy, Chem. A Eur. J. **23**, 16004 (2017).
[25]P. Stoliar, L. Cario, E. Janod, B. Corraze, C. Guillot-Deudon, S. Salmon-Bourmand, V. Guiot, J. Tranchant, and M. Rozenberg, Adv. Mater. **25**, 3222 (2013).
[26]V. Guiot, L. Cario, E. Janod, B. Corraze, V. Ta Phuoc, M. Rozenberg, P. Stoliar, T. Cren, and D. Roditchev, Nat. Commun. **4**, 1722 (2013).
[27]F. Pan, S. Gao, C. Chen, C. Song, and F. Zeng, Mater. Sci. Eng. R Rep. **83**, 1 (2014).
[28]L. Cario, C. Vaju, B. Corraze, V. Guiot, and E. Janod, Adv. Mater. **22**, 5193 (2010).
[29]M. Querré, J. Tranchant, B. Corraze, S. Cordier, V. Bouquet, S. Députier, M. Guilloux-Viry, M.-P. Besland, E. Janod, and L. Cario, Phys. B Condens. Matter **536**, 327 (2018).
[30]P. Diener, E. Janod, B. Corraze, M. Querré, C. Adda, M. Guilloux-Viry, S. Cordier, A. Camjayi, M. Rozenberg, M.-P. Besland, and L. Cario, Phys. Rev. Lett. **121**, 016601 (2018).
[31]F. Tesler, C. Adda, J. Tranchant, B. Corraze, E. Janod, L. Cario, P. Stoliar, and M. Rozenberg, "Relaxation of a Mott-neuron," Phys. Rev. Appl. (to be published); e-print arXiv:1711.05206 [cond-mat] (2017).
[32]L. Lapicque, Biol. Cybern. **97**, 341 (2007).
[33]L. Lapicque, J. Physio. Patho. Générale **9**, 567 (1907).
[34]A. Tavanaei, M. Ghodrati, S. R. Kheradpisheh, T. Masquelier, and A. S. Maida, e-print arXiv:1804.08150 [Cs] (2018).
[35]C. Adda, L. Cario, J. Tranchant, E. Janod, M.-P. Besland, M. Rozenberg, P. Stoliar, and B. Corraze, MRS Commun. **8**, 835 (2018).